Interferometric detection of pressure field developing around nanosecond discharge filaments in deionized water

Petr Hoffer, Václav Prukner, Jiří Schmidt, Milan Šimek

Institute of Plasma Physics of the CAS, Prague, Czech Republic

Abstract: Spatially-resolved pressure field produced by ns discharges in deionized liquid water around a needle anode was investigated by picosecond laser interferometry. The changes of the refractive index produced a shift of fringes in interference patterns, which evidences shockwaves associated with propagating filaments. However, in some cases, very thin streamer channels (diameter of ~1 μm) were captured with no fringes, suggesting a stepwise propagation mechanism of discharge filament with/without associated shockwaves.

Keywords: nanosecond, discharge, water, interferometry.

1. Introduction

Generation of shockwaves by spark discharges in liquid water is a well-known phenomenon with important practical applications (e.g. in shockwave lithotripsy). However, shockwaves are generated also by low current corona-like discharges. In the case of discharges emanating from positive electrode, non-luminous *primary streamers* are often the initial phase of plasma propagation in water, which can, but need not start to propagate from an initial gas bubble with plasma streamers inside. The launch of primary streamers is triggered, when local electric field is of the order of 100 MV·m^{-1} [1]. Propagation of primary streamers is often accompanied by a phase transition, occurrence of microbubbles, and their hydrodynamic expansion. Primary discharges have hemispherical bush-like appearance, where the edges of the individual streamers can be clearly resolved (their channel diameters were measured to be 3-10 µm [2]), and propagate along radial directions at relatively low velocities (often subsonic, but some may reach even several kilometers per second) producing spherical shockwaves. Therefore, the initial disturbance has approximately spherical shape. Adjacent electric field may initiate subsequent discharges or produce gaseous bubbles in the bulk liquid and thus elongate the streamer channel. The process stops when the breakdown voltage of the gaseous channel becomes higher than the voltage along the channel or when the electric field at the active tip of one of the streamer becomes so high that *secondary streamers* can be formed [3] [1] [4]. The secondary streamers often start out of the primary streamers and they are much more luminous [5, 6]. However, under specific conditions, streamer channels can be produced directly. Secondary streamers have a filamentary structure (channel diameters significantly larger than that of the primary streamers, roughly in the 5–25 µm range), and propagate much faster than the primary streamers. The propagation velocity of secondary streamers ranges from a few kilometers per second up to about 500 km·s^{-1} (depending on the high-voltage waveform and electrode geometry) [2]. Field-induced dissociation and ionization of water molecules in the bulk liquid are considered as main mechanisms for secondary streamer propagation, because electric field around secondary streamer heads reaches about 2 GV·m^{-1} [1]. The ion mobility in the liquid vapor in the streamer channel gives drift velocities of the order of 10^3 m·s^{-1} for heavy ions and 10^5 m·s^{-1} for protons, the main product of the water dissociation and ionization. The vaporization at the tip of a streamer head thus also takes place due to charged particle flow from the discharge plasma in the streamer channel (fast energy input into the water volume). This argument is based on the fact, that the discharge input energy is consistent with the energy required to vaporize the volume of water contained in the streamer channels [5] The phase transition requires increase of liquid specific volume, which is accompanied by production of shockwaves [4]. However, at the nanosecond time scale a more probable scenario should be taken into account, as it is implied in the section of experimental results.. Since the mechanism of the Townsend breakdown in water vapor is independent on the water conductivity, the streamer velocity also does not depend on the water conductivity.

Pressure distribution around positive secondary streamers was studied in more detail in [1] by means of Mach-Zehnder interferometry. Evaluation of fringe shifts in produced interference patterns of the streamer surroundings allow estimation of the pressure profile, since the fringe shift represents a phase shift due to deviations of the liquid refractive index (which is a known function of the liquid pressure at given temperature). Streamers can be recognized by the conical shape (Mach cone) of the shock front evolving from them. At driving voltage of 20 kV, the peak pressure of the shock front, when it reached radius of 35 µm, was 46 MPa. A reproduction of the detected pressure field required 2–3 ns pressure pulses with amplitudes of up to 5.8 GPa [6, 1].

Another approach to evaluate the shock-front pressure is described in [6], where high-speed shadowgraphy was utilized to determine speed of the shock-front. The shock-front speed was directly related to the shock-front pressure. At the driving voltage of 15 kV, the maximum shock velocity reached 4.2 km·s^{-1}, which, according to the authors, corresponded to initial pressure of 5.8 GPa inside the plasma channel. Although the regression was performed at constant liquid density, this value was comparable to that obtained in [1].

The main purpose of experiments described in this work is to develop suitable setup for the pressure field measurement in vicinity of nanosecond positive corona-like discharges produced in distilled water.

2. Experimental setup

The experimental setup of the experiment is depicted in Fig. 1a. The pulsed power supply (FID nanosecond pulser) produced HV pulses +100 kV/10ns. The pulsed source was connected to the tungsten needle anode, where corona streamers were produced. Deionised water (~1 μS/cm) was used as working liquid. The compact discharge chamber is sketched in Fig. 1b.

The concept of a modified Mach-Zehnder interferometer was used to detect the pressure field. Since water refractive index (~1.334) is higher than that of the air (~1) the probing laser beam touching the needle electrode is significantly delayed. Therefore, it was necessary to delay also the reference beam. Guiding the reference beam through the same discharge chamber (but sufficiently far from the needle tip) enabled placing the second beam splitter in such a way that we could place the projecting lens very close to the output window of the chamber.

The Katana 05 (Onefive) laser (532 nm/30 ps/4 nJ) was used to produce probe and reference beams. The CMOS camera (Canon 760D, 24 MPx) was used as detector. The diameter of the output window and the output beam-splitter of the interferometer was 50 mm.

3. Results

Generally, optical interferometry is based on interference of reference (direct) and probing (propagating through the analyzed optical inhomogeneity) light rays characterized with different phases. The phase shift is due to propagation through regions with different refraction indexes. The constructive/destructive interference leads to creation of bright and dark regions on the plane of CCD chip of the camera. When mirrors and beam splitters of the interferometer are adjusted appropriately and when both the reference and probe beams propagate through optically homogeneous environment, then the interference pattern contains parallel fringes with adjustable pitch only [7]. Any optical inhomogeneity in the path of interfering beams results in a shift of fringes; this shift can be used for evaluation of the phase shift in each point of the interference pattern. Since interferograms provide information about deviations of the refractive index inside an inhomogeneity, it is possible to calculate profile of liquid density and hence, the appropriate pressure profile.

Typical examples of interference patterns captured in present experiments are shown in Fig. 2. Fig. 2a shows areas with no visible fringes. This means that the probing laser beam did not match the field of view of the optical detection system due to presence of many opaque streamers; the interference pattern could not have been constructed there. Figures Fig. 2b,c show highly magnified areas around tips of the streamers. Sharp shift of the fringes in the Fig. 2b evidences presence of shockwaves produced by streamers, which were hardly visible in the interferograms. The Fig. 2c illustrates a very thin structure (about 1.4 μm in diameter) with no visible fringes. If it was a streamer channel, then one would expect presence of a shockwave around it, a pressure field of a structure similar to that seen in the Fig. 2b. Alternative explanation is that it is a very early streamer channel, which was captured just after its formation. Such a channel could be very thin, formed with supercritical water at high pressure and temperature, and surrounded by high-pressure shockwave with diameter of 1.4 μm. No interference pattern can be seen in the area, since the measuring laser beam was bent outside of the field of view of the optical system by the very strong optical inhomogeneity. This scenario is quite possible considering much higher propagation speed of streamers (100-1000 km/s) in comparison with typical shockwaves in water (1.5-10 km/s).

In the future, we will capture and analyze interferograms with varying time delay with respect to the high-voltage waveform. They will be used to estimate the pressure distribution developing around streamers with visible fringe shifts. Particular attention will be paid to the “dark” streamers without any fringe shifts.

Acknowledgement

This work was supported by the Czech Science Foundation under project No. 18-04676S.

4. References

[1] W. An, K. Baumung and H. Bluhm, "Underwater Streamer Propagation Analyzed from Detailed Measurements of Pressure Release," *J. Appl. Phys.,* vol. 101, p. 053302(10), 2007.

[2] J. F. Kolb, R. P. Joshi, S. Xiao and K. H. Schoenbach, "Streamers in Water and Other Dielectric Liquids," *J. Phys. D: Appl. Phys.,* vol. 41, p. 234007 (22), 2008.

[3] P. Bruggeman and C. Leys, "Non-thermal Plasmas in And in Contact with Liquids," *J. Phys. D: Appl. Phys.,* vol. 42, p. 053001(28), 2009.

[4] V. Y. Ushakov, Impulse Breakdown of Liquids, Heidelberg: Springer-Verlag, 2007.

[5] M. Šimek, M. Člupek, V. Babický, P. Lukeš and P. Šunka, "Emission Spectra of a Pulse Needle-to-Plane Corona-Like Discharge in Conductive Aqueous Solutions," *Plasma Sources Sci. Technol.,* vol. 21, p.

055031 (12), 2012.

[6] M. Šimek, B. Pongrác, V. Babický, M. Člupek and P. Lukeš, "Luminous phase of nanosecond discharge in deionized water: morphology, propagation velocity and optical emission," *Plasma Sources Sci. Technol.*, vol. 26, p. 07LT01, 2017.

[7] I. V. Lisitsyn, H. Nomiyama, S. Katsuki and H. Akiyama, "Thermal Processes in a Streamer Discharge in Water," *IEEE Transactions on Dielectrics and Electrical Insulation*, vol. 6, pp. 351-356, 1999.

[8] I. Marinov, S. Starikovskaia and A. Rousseau, "Dynamics of plasma evolution in a nanosecond underwater discharge," *J. Phys. D: Appl. Phys.*, vol. 47, p. 224017 (10pp), 2014.

[9] B. Gross, Měření vysokých teplot, Praha: SNTL, 1962.

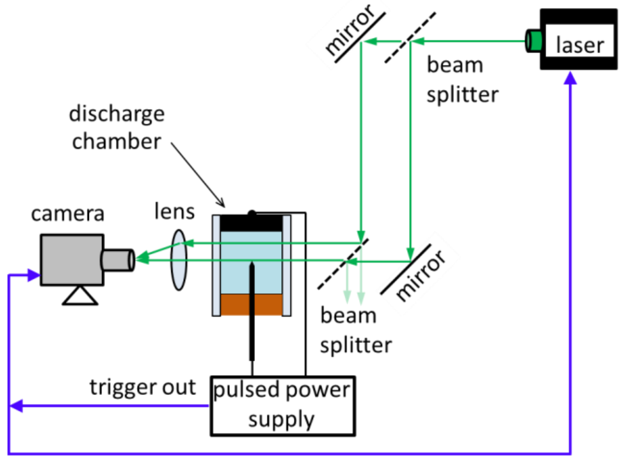

a)

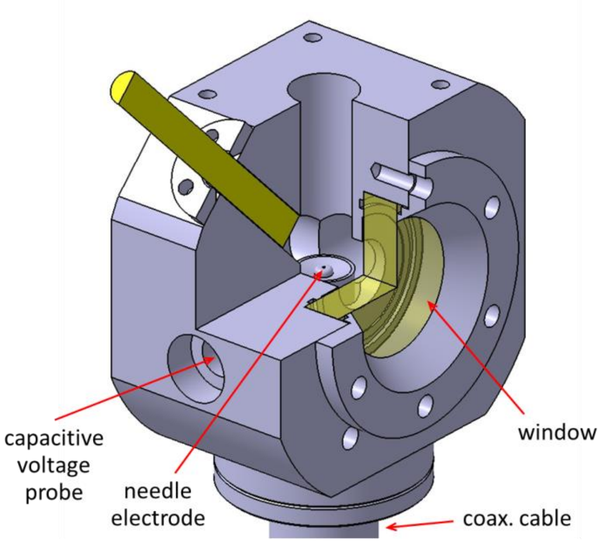

b)

Fig. 1 Experimental setup.

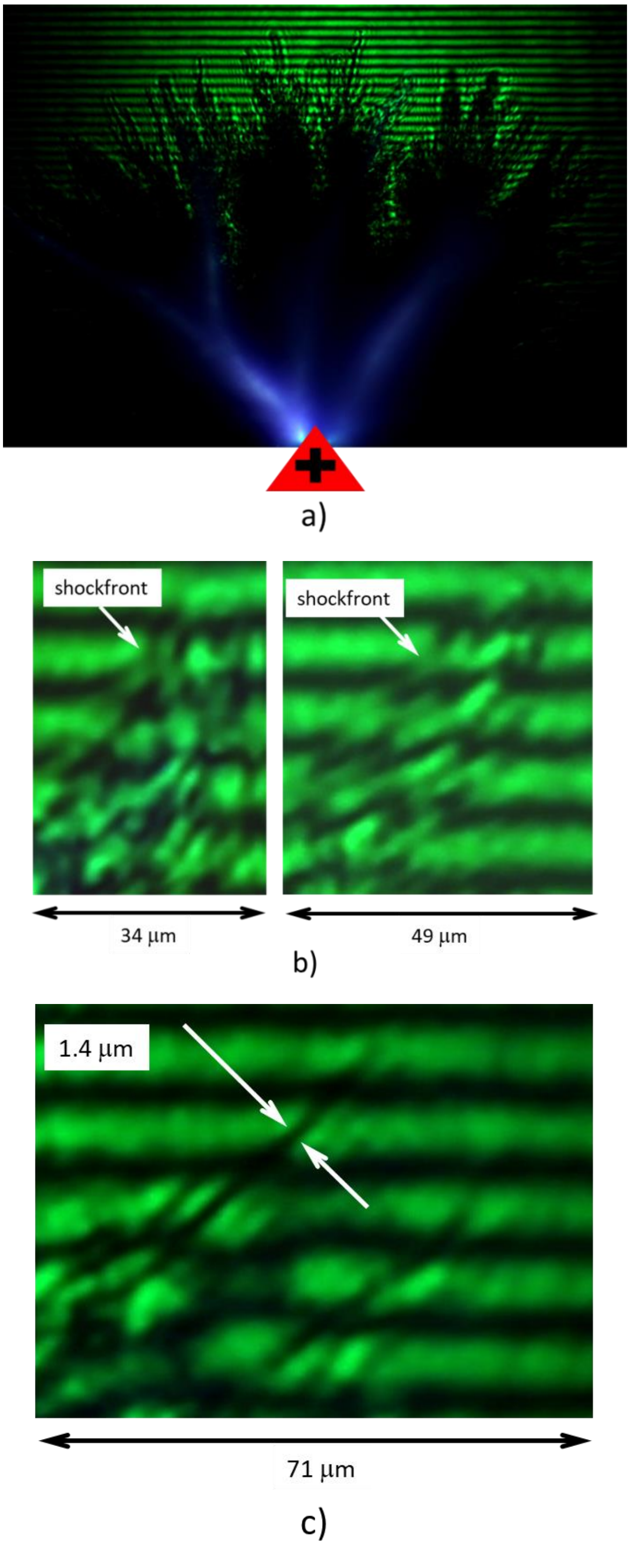

Fig. 2 Examples of captured interferograms.